

Short communication

Metal-doped $\text{Li}_2\text{Ti}_3\text{O}_7$ with ramsdellite structure as high voltage anode for new generation Li-ion batteries

M. Van Thournout^a, L. Aldon^{a,*}, M. Womes^a, B. Ducourant^a,
J. Olivier-Fourcade^a, C. Tessier^b, S. Levasseur^c

^a *Laboratoire des Agrégats Moléculaires et Matériaux Inorganiques (CNRS–UMR 5072), Université Montpellier II, CC015, Place Eugène Bataillon, 34095 Montpellier cedex 5, France*

^b *SAFT—Direction de Recherche, 111 Bd Alfred Daney, 33074 Bordeaux cedex, France*

^c *UMICORE—Research and Development, Kasteelstraat 7, 2250 Olen, Belgium*

Available online 26 June 2007

Abstract

$\text{Li}_2\text{Ti}_3\text{O}_7$ is considered to be a promising insertion material for high power battery applications because of its open structure with accessible vacancies. High-rate cycling ($C/10$ and $1.5C$) has been performed and results show small irreversibility and low polarisation, but capacity losses are noticed during cycling. Partly substituting Ti^{IV} with Fe^{III} improves the cyclability but a significant irreversible part is obtained due to the participation of iron in the insertion mechanism. This additional reduction level lowers with a combination of two transition elements, Fe and Ni, on the ramsdellite framework sites. Moreover, lower polarisation and higher capacities are observed.

In this work, Ti^{IV} and Li are partly replaced by a combination of three elements (Fe^{III} , Ni^{II} and Al^{III}) in order to further improve the electrochemical performances. The difference in charge balance is obtained by metal and oxygen vacancies, which implies new vacancies and a better accessibility to the existing vacancies for lithium insertion. Several characterisation methods have been used on three different samples (Fe, Fe/Ni and Fe/Ni/Al), which made it possible to observe wider channels in the distorted ramsdellite lattice. In this case, lithium ions circulate more easily into the channels resulting in better reversibility upon cycling, which is necessary for high-rate cycling.

© 2007 Elsevier B.V. All rights reserved.

Keywords: Ramsdellite structure; Substitution; Lithium ion insertion; High-rate cycling

1. Introduction

The increasing demand for high-energy storage devices for high power applications, such as hybrid electric vehicles, leads to the development of new generation Li-ion accumulators. Such a demand requires a safe system with low toxic and less expensive electrode materials. Today, carbon/graphite negative electrodes are used in lithium cells currently on the market, but this type of anode is not really appropriate for high-power applications (risk of explosive events). Some safety problems can be solved by replacing the carbon/graphite negative electrode by high voltage insertion materials with a working potential between 1 and 2 V. Lithium titanium oxides fulfil these requirements [1,2]. $\text{Li}_4\text{Ti}_5\text{O}_{12}$ and $\text{Li}_2\text{Ti}_3\text{O}_7$ are known to be good ionic conductors which do not suffer from high volume expansion during

lithium insertion. A few years ago, a new type of lithium cell based on the combination of a spinel structure, i.e. $\text{Li}_4\text{Ti}_5\text{O}_{12}$ anode and a high voltage cathode was proposed [3,4]. Recently, transition metal-doped titanates have drawn attention in order to investigate the relationship between structure and electrochemical properties [5,6]. In addition, it has been shown earlier that a lower synthesis temperature and a better cyclability can be achieved by substituting a small amount of Ti^{4+} with Fe^{3+} in $\text{Li}_2\text{Ti}_3\text{O}_7$, even though poor capacity values are obtained [7]. However, the first discharge curve shows a plateau due to the reduction of Fe^{3+} to Fe^{2+} , which restricts the reversible capacity. Therefore, it is interesting to keep working on the improvement of the electrochemical properties of the substituted $\text{Li}_2\text{Ti}_3\text{O}_7$ ramsdellite phase. In this paper, three metals – Fe^{3+} , Ni^{2+} and Al^{3+} – have been chosen in order to both stabilise the ramsdellite lattice and increase ionic and electronic conductivity [8]. Several structural characterisation methods will be presented along with the electrochemical properties and cycling behaviour at high current densities.

* Corresponding author.

E-mail address: laldon@univ-montp2.fr (L. Aldon).

2. Experimental

Three ramsdellite compounds have been synthesized by partly substituting (A) $\text{Ti}^{4+}/\text{Li}^+$ by Fe^{3+} , or (B) Fe^{3+} and Ni^{2+} (ratio 1:4), or (C) Fe^{3+} , Ni^{2+} and Al^{3+} (ratio 1:4:1), using the conventional ceramic synthesis route from pure oxides available on the market: Li_2CO_3 , TiO_2 , Fe_2O_3 , NiO and Al_2O_3 . The precursors were ground homogeneously by planetary ball milling and heat treated at 980°C followed by quenching to stabilise the ramsdellite structure. Alternatively, sample B has been enriched in the ^{57}Fe isotope by a sol–gel process in order to insert a probe for ^{57}Fe Mössbauer spectroscopy. The samples were characterised by X-ray powder diffraction (XPD) with a Phillips θ – 2θ diffractometer using $\text{Cu K}\alpha$ radiation and nickel filter.

Electrochemical lithiation was performed in SwagelokTM test cells using the synthesized samples as positive electrodes containing carbon black and polytetrafluoroethylene (PTFE) as binder (ratio 80:10:10). The mixture was then pressed to obtain the shape of a pellet. Metallic lithium was used as the counter electrode and 1 M LiPF_6 in a mixture of ethylene carbonate (EC), propylene carbonate (PC) and dimethylene carbonate (DMC) (v/v 1:1:3) was used as the electrolyte. The battery was assembled in an argon-filled glove box. Galvanostatic discharge/charge curves were obtained using a McPile II system at constant current densities, 10 mA g^{-1} (C/10) and 149 mA g^{-1} (1.5C).

Samples A and B have been characterised by ^{57}Fe Mössbauer spectroscopy at room temperature with a standard EG and G accelerator spectrometer in transmission mode using a ^{57}Co in Rh matrix as the γ -ray source. ^{57}Fe hyperfine parameters are determined by fitting Lorentzian curves to the experimental data [9].

Neutron diffraction was carried out at Institut Laue-Langevin, Grenoble, France, using powder diffractometer D1B ($\lambda = 1.2806\text{ \AA}$). Structural refinements were carried out using the Rietveld method with the WinplotR/Fullprof package [10].

3. Results

3.1. Structural characterisation

Several characterisation methods have been used in order to acquire a better knowledge of the crystalline structure.

One of the features of the $\text{Li}_2\text{Ti}_3\text{O}_7$ ramsdellite compound (Pbnm space group) is to be an open structure with channels, which makes Li^+ ion diffusion possible. From neutron diffraction, we previously reported a structural formula intermediate to those proposed by Morosin and Mikkelsen [11] $[\text{Li}_{1.77}\square_{2.23}]_c[\text{Ti}_{3.43}\text{Li}_{0.52}\square_{0.05}]_f\text{O}_8$ (\square = vacancies, c = channel, f = framework) in a paper, which presumes vacancies in both the tetrahedral sites in the channels and the octahedral sites in the framework [12]. In that paper, we reported about the cation distribution of two iron-doped compounds (Ti/Fe=9), one with an excess of lithium in the channels and one with oxygen vacancies. In both cases, all framework sites were occupied by Ti, Fe and Li (no vacancies left), but the compound with oxygen vacancies showed more

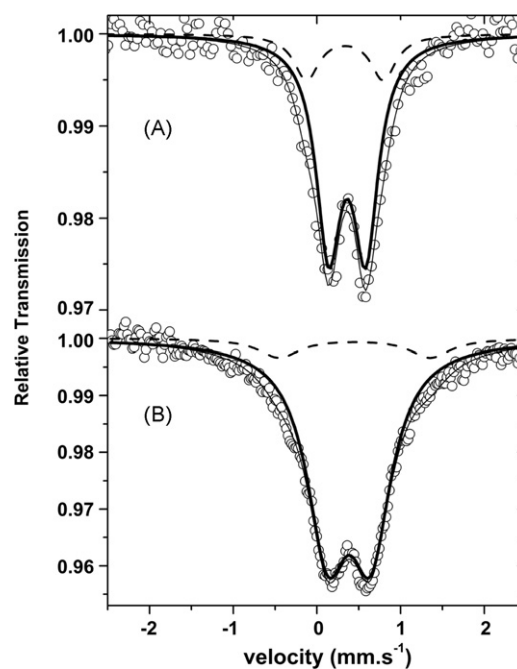


Fig. 1. Room temperature ^{57}Fe Mössbauer spectra of (A) Fe-doped and (B) Fe–Ni doped samples.

channel sites available for lithium insertion than the compound containing too much lithium. This was in good agreement with the synthesis conditions.

^{57}Fe Mössbauer spectroscopy has been carried out on sample A with Ti/Fe = 9 and sample B (Fig. 1), both having oxygen vacancies. Refined isomer shifts and quadrupole splittings correspond to iron atoms located in octahedral sites with a Fe^{III} oxidation state (Table 1). For both samples, two subspectra are observed, which evidences two different environments of the probed iron atom. The large quadrupole splitting observed in sample B is related to the probability of finding Li, Ti, Fe, Ni and O atoms or oxygen vacancies in the framework which is made up of the nearest neighbours of the probed iron atoms. This reveals more distorted octahedra and inhomogeneous environments of iron in this case.

In this work, we report about the structural effects on the electrochemical performances of the materials after a 5% Ti substitution by one (Fe) (A), two (Fe, Ni) (B) or three (Fe, Ni, Al) (C) metal elements. Charge balance is obtained by oxygen vacancies. These three elements have been chosen because of their ionic radius between 0.5 and 0.8 Å, close to that of Ti^{4+}

Table 1
Room temperature ^{57}Fe hyperfine parameters of (A) Fe doped and (B) Fe–Ni doped samples

Sample	IS (mm/s)	QS (mm/s)	2Γ (mm/s)	A%	Attribution
A	0.36 (1)	0.44 (1)	0.36 (2)	82	Fe^{III} octa
	0.33 (3)	0.92 (5)	0.36 (10)	18	Fe^{III} octa
B	0.38 (1)	0.52 (1)	0.60 (1)	91	Fe^{III} octa
	0.45 (4)	1.80 (6)	0.60 (12)	9	Fe^{III} octa

Isomer shifts (IS) are given to α -Fe; QS, quadrupole splitting; 2Γ , the line width at half maximum; A%, the contribution of sub-spectra to the spectrum.

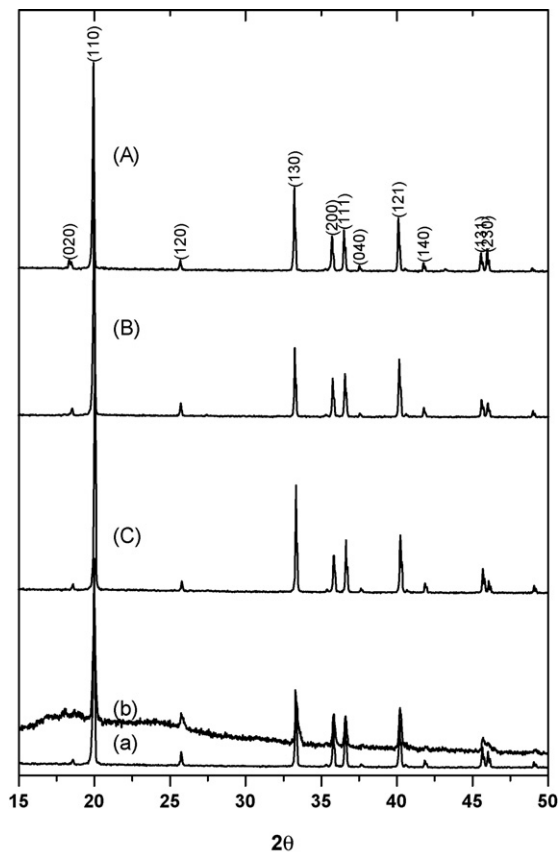


Fig. 2. X-ray diffraction patterns of $\text{Li}_2\text{Ti}_3\text{O}_7$ ramsdellite before (a) Li insertion and (b) after insertion of $x = 1.4$ Li. (A) Compounds doped with Fe, (B), Fe–Ni and (C) Fe–Ni–Al.

(0.60 Å) and for their ability to form an octahedral structure with oxygen.

A pure ramsdellite phase can be observed from the X-ray diffraction patterns for each compound (Fig. 2). We have found, by substituting different amounts of heavier metals, that some impurities may be noticed (Li_2TiO_3 , TiO_2 rutile). The unit cell dimensions, reported in Table 2, are in good agreement with those of the pristine compound. The column $a \times b$ represents the dimension of a channel. As can be seen in the table, the channel size slightly increases due to the different ionic radii of the substituted elements in the ramsdellite framework.

3.2. Electrochemical tests

Fig. 3 shows the discharge–charge profiles of the three synthesized samples down to 1 V at a 10 mA g^{-1} constant current density. We observe that the three curves have an “S”-shaped

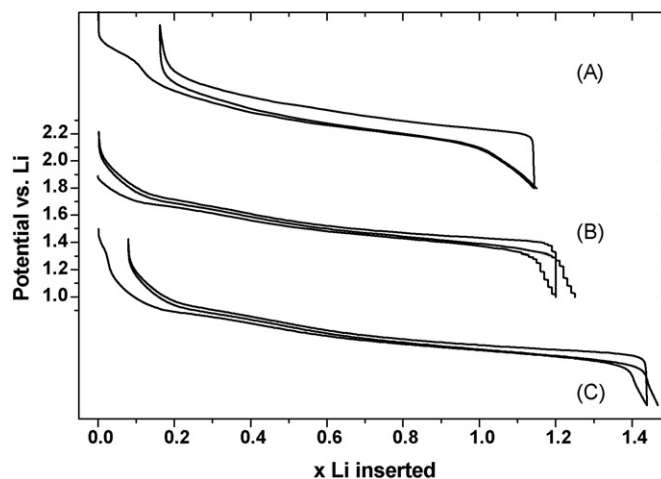


Fig. 3. First discharge curve of samples A, B and C at a current density of 10 mA g^{-1} .

profile, which is a feature of one-phase insertion mechanisms of lithium, without altering the host compound.

The iron-doped sample (sample A) shows the $\text{Fe}^{3+}/\text{Fe}^{2+}$ shoulder between 1.8 and 2.1 V. Irreversibility after the first charge increases and the capacity values are lower compared to those obtained for the pristine compound. To avoid this extra reduction, the addition of Ni^{2+} to Fe^{3+} (ratio 4:1) eliminates the $\text{Fe}^{3+}/\text{Fe}^{2+}$ voltage step, assuming electron exchange between iron and nickel [13]. Furthermore, excellent cyclability is maintained with increasing capacities. Variations in reversible capacity according to the number of cycle for samples A, B and C are plotted at 1.5C showing good cycling capabilities during 50 cycles (Fig. 4).

In iron-doped samples, the size of the channels is bigger than in the undoped pristine $\text{Li}_2\text{Ti}_3\text{O}_7$. The origin of the lower reversible capacity may be due to a lower ionic conductivity and/or presence of iron in the channels limiting accessibility of Li in the structure.

4. Discussion

$\text{Li}_2\text{Ti}_3\text{O}_7$ is regarded as a promising negative electrode material due to its excellent ionic conductivity, volume expansion (only 2%), excellent reversibility during charge and discharge and low polarisation [14]. The vacancies available in the channels make it possible to insert 2.28 lithium which correspond to a theoretical capacity of 198 mA h g^{-1} . Assuming that all the Ti^{4+} can be reduced to Ti^{3+} , the theoretical capacity should be 298 mA h g^{-1} [2]. But because of the two different intercalation sites and a short Li–Li distance (~ 1 Å), only one site out of

Table 2

Cell parameters (a , b , c) of the doped ramsdellite structures with corresponding channel size ($a \times b$) compared to the pristine compound

Composition	a (Å)	b (Å)	c (Å)	$a \times b$ (Å ²)
$\text{Li}_{16/7}\text{Ti}_{24/7}\text{O}_8$	5.017 (1)	9.556 (1)	2.947 (1)	47.94 (1)
(A) $\text{Li}_{16/7}\text{Ti}_{(3-x)/8/7}\text{Fe}_{x/8/7}\text{O}_{(7-x/2)/8/7}$ ($x = 0.15$)	5.017 (1)	9.570 (2)	2.950 (1)	48.01 (2)
(B) $\text{Li}_{(2-x)/8/7}\text{Ti}_{(3-5x)/8/7}\text{Fe}_{x/8/7}\text{Ni}_{(4x)/8/7}\text{O}_{(1-x)/8}$ ($x = 0.03$)	5.014 (1)	9.571 (1)	2.946 (1)	47.99 (1)
(C) $\text{Li}_{(2-6x)/8/7}\text{Ti}_{(3-6x)/8/7}\text{Fe}_{x/8/7}\text{Ni}_{(4x)/8/7}\text{Al}_{x/8/7}\text{O}_{(1-x)/8}$ ($x = 0.025$)	5.014 (1)	9.568 (1)	2.946 (1)	47.97 (1)

Table 3

Initial capacity, reversibility upon the first cycle and polarisation for the three proposed ramsdellite compounds at two different regimes

Composition	10 mA g ⁻¹			149 mA g ⁻¹		
	Initial capacity (mAh g ⁻¹)	Efficiency (%)	Polarisation	Initial capacity (mAh g ⁻¹)	Efficiency (%)	Polarisation
Li _{16/7} Ti _{24/7} O ₈	141	95	69 mV	110	98	313 mV
(A) (x=0.15)	114	86	95 mV	85	81	319 mV
(B) (x=0.03)	139	91	37 mV	105	94	266 mV
(C) Li (x=0.025)	145	94	34 mV	109	95	221 mV

two can be occupied [15]. However, higher capacities have been found, about 235 mAh g⁻¹, under open-circuit-voltage (OCV) down to 1 V [14].

We are more interested in cycling behaviour at higher and constant current densities. Garcia-Alvarado et al., found that, at cycling rate C/10, the ramsdellite compound maintained acceptable specific capacity values, 129 mAh g⁻¹, though they have not performed long-life cycling behaviour experiments [16].

The aim of substituting less charged metal elements in titanium sites allows us to stabilise the ramsdellite lattice and create more vacancies in the channels in order to improve the electrochemical performances [12,13]. Indeed, as shown in Fig. 4 and Table 3 the following improvements are obtained: an increase in specific capacity and efficiency after the first cycle, a good stability and quite satisfactory capacity values are obtained at a fast cycling rate (1.5C) for samples B and C. Moreover, for both samples, lower and stable polarisation is obtained.

Only iron doping shows large irreversibility after the first cycle due to a first insertion mechanism of lithium which converts Fe³⁺ into Fe²⁺. This phenomenon has been confirmed by ⁵⁷Fe Mössbauer spectroscopy. Different spectra have been recorded *ex situ* at the end of a discharge and a charge cycle [17]. Both spectra showed 100% of Fe^{II}, assuming that the reversible cycling behaviour only works during the Ti⁴⁺/Ti³⁺ redox process, which restricts the lithium insertion mechanism.

The co-doped ramsdellite phases (B and C) are obtained with less lithium; furthermore larger channel widths are noticed (Table 2). The improvements of the electrochemical performances seem to go along with either an increasing number of

possible sites for the inserted lithium or by making the accessibility to the existing sites easier. The second assumption seems more acceptable given that, for the iron-doped compound, large channels are also obtained but the capacity values are lower. The key issue in this case is the limitation of lithium mobility.

It seems that the combination of two and three substitutions in the ramsdellite structure further stabilises the host network, releases diffusion paths for lithium through the channels and increases ionic and electronic conductivity in order to increase specific power.

5. Conclusion

Partial substitution of Li and Ti (from the Li₂Ti₃O₇ compound) in addition to Fe atoms in octahedral sites with one or two other elements, i.e. Ni and Al, has been studied. A more stable ramsdellite structure is obtained at lower synthesis temperatures.

The observation of larger channels seems to improve the ionic conductivity. Furthermore, the electrochemical performances are improved with excellent reversibility, acceptable capacity values at 1.5 C rate and high efficiency upon cycling.

The difference in charge balance also improves electronic conductivity as the polarisation of the co-doped (Fe, Ni, Al) Li₂Ti₃O₇ is considerably improved.

This type of anode material can be associated with high voltage positive material in future new-generation lithium ion batteries.

Acknowledgements

The authors are grateful to SAFT (France) and UMI-CORE (Belgium) for financial support, CNRS-UMII-SAFT-UMICORE convention No. 752964/00. They are also thankful to Pierre Strobel and Olivier Isnard from Laboratoire de Cristallographie CNRS (Grenoble, France) for measurements and analyses of neutron diffraction.

References

- [1] T. Ohzuku, A. Ueda, N. Yamamoto, J. Electrochem. Soc. 142 (1995) 1431.
- [2] R.K.B. Gover, J.R. Tolchard, H. Tukamoto, T. Murai, J.T.S. Irvine, J. Electrochem. Soc. 146 (1999) 4348.
- [3] S. Panero, M. Satolli, M. Salomon, B. Scorsati, Electrochem. Comm. 2 (2000) 810.
- [4] A.N. Jansen, A.J. Kahaian, P.A. Nelson, K. Amine, D.W. Dees, D.R. Visers, M.M. Thackeray, J. Power Sources 81/82 (1999) 902.
- [5] A.D. Robertson, L. Trevino, H. Tukamoto, J.T.S. Irvine, J. Power Sources 81/82 (1999) 352.

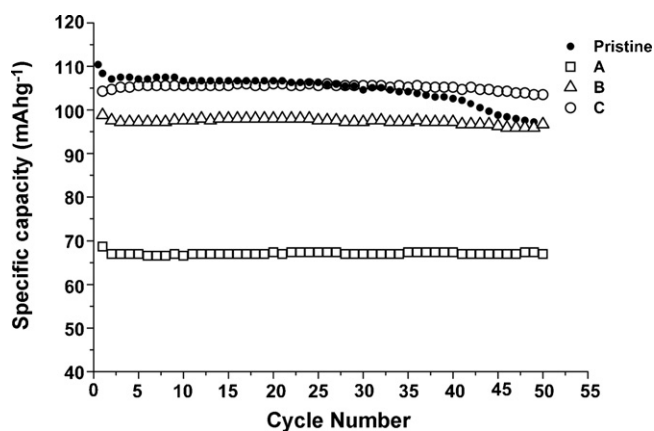


Fig. 4. Specific charge capacity values as a function of the number of cycle obtained at current density 149 mA g⁻¹ for the pristine compound (solid circles), samples A (squares), B (triangles) and C (open circles).

- [6] P. Kubiak, A. Garcia, M. Womes, L. Aldon, J. Olivier-Fourcade, P.E. Lippens, J.C. Jumas, *J. Power Sources* 119–121 (2003) 626.
- [7] S. Ma, H. Noguchi, *Electrochemistry* 69 (2001) 526.
- [8] J.C. Jumas, J. Olivier-Fourcade, P.-E. Lippens, L. Aldon, A. Picard, P. Kubiak, International Application Published under the Patent Cooperation Treaty (PCT); WO2004/100292, 2004.
- [9] K. Ruebenbauer, T. Birshall, *Hyperfine Interact.* 7 (1979) 125.
- [10] J. Rodriguez-Carvajal, *Physica B* 192 (1993) 55.
- [11] B. Morosin, J.C. Mikkelsen Jr., *Acta. Cryst. B*35 (1979) 798.
- [12] L. Aldon, M. Van Thournout, P. Strobel, O. Isnard, J. Olivier-Fourcade, J.C. Jumas, *Solid State Ionics* 177 (2006) 1185.
- [13] M. Van Thournout, A. Picard, M. Womes, J. Olivier-Fourcade, J.C. Jumas, *J. Phys. Chem. Solids* 67 (5–6) (2006) 1355.
- [14] M.E. Arroyo de Dompablo, E. Moran, A. Varez, F. Garcia-Alvarado, *Mater. Res. Bull.* 32 (1997) 993.
- [15] S. Garnier, C. Bohnke, O. Bohnke, J.L. Fourquet, *Solid State Ionics* 83 (1996) 323.
- [16] F. Garcia-Alvarado, M.E. Arroyo de Dompablo, E. Moran, M.T. Gutierrez, A. Kuhn, A. Varez, *J. Power Sources* 81/82 (1999) 85.
- [17] L. Aldon, P. Kubiak, A. Picard, P.E. Lippens, J. Olivier-Fourcade, J.C. Jumas, *Hyperfine Interact.* 156/157 (2004) 497.